PCCP

Accepted Manuscript

ROYAL SOCIETY OF CHEMISTRY

www.rsc.org/pccp

Critical Temperature and Products of Intrachain Polaron Recombination in Conjugated Polymers

Wiliam Ferreira da Cunha†, Luiz Antonio Ribeiro Junior‡,* Ricardo Gargano†, and Geraldo Magela e Silva††

† *Institute of Physics, University of Brasilia, 70.919-970, Brasilia, Brazil and*

‡ *Department of Physics, Chemistry and Biology (IFM), Linköping University, SE-581 83 Linköping, Sweden*

(Dated: June 27, 2014)

Abstract

The intrachain recombination dynamics between oppositely charged polarons is theoretically investigated through the use of a version of the Su-Schrieffer-Heeger (SSH) model modified to include an external electric field, extended Hubbard Model, Coulomb interactions, and temperature effects in the framework of a nonadiabatic evolution method. Our results indicate notable characteristics concerning the polaron recombination: (1) it is found that there exist a critical temperature regime, below which an exciton is formed directly and (2) a pristine lattice is the resulting product of the recombination process, if the temperature is higher than the critical value. Additionally, it is obtained the critical electric field regime that played the role of drastically modifying the system dynamics. These facts suggest that thermal effects in the intrachain recombination of polarons are crucial for the understanding of electroluminescence in optoelectronics devices, such as Polymer Light Emitting Diodes.

Keywords: Su-Schrieffer-Heeger Model, Recombination, Polaron, Exciton, Conjugated Polymers.

*Electronic address: luiju@ifm.liu.se

†Electronic address: magela@fis.unb.br

I. INTRODUCTION

Since the discovery of poly(paraphenylene vinylene) (PPV) and its electroluminescence properties, considerable amounts of effort has been devoted to study the photophysical applications of conjugated polymers for development of new technologies in organic opto-electronic devices. The potential advantages in terms of ease of synthesis, flexibility, low cost, and large-area capability make these materials attractive for the electronics industry, particularly when it comes to the promising development of a new display technology. This kind of system has been successfully implemented as the active component in various applications such as Organic Photovoltaics devices (OPVs) [1] and Polymer Light Emitting Diodes (PLEDs) [2]. In these devices, the generation of excited states is the fundamental physical process involved. Particularly, polaron recombination is the key step behind the mechanism of electroluminescence in PLEDs. It is well known that when two polarons with opposite charges overlap in space, they will collide and recombine to form new species. The photon emission phenomena depends sensitively on the radiative decay of excited species, which are formed from the reaction between the charge carriers. A considerable amount of theoretical work, focused on understanding the processes underlying excited states formation in conjugated polymers through the collision mechanism of oppositely charged carriers, has been performed in the last years [3–11]. Nevertheless, studies that take into account the temperature influence on such mechanisms remains not available theoretically and are also very difficult to control experimentally.

Recently, An and coworkers used the Su-Schrieffer-Heeger (SSH) model to simulate the polaron recombination process in conjugated polymers [4]. The goal was to identify the generation mechanism of the self-trapped polaron-exciton when only electric field effects are taken into account. Their results show that there are three regimes of the applied electric field to form new species. Li *et al.* [11] simulated the same process by adding Hubbard type electron-electron interactions to the SSH Hamiltonian. The simulations have pointed out that two polarons can recombine directly and efficiently in a full exciton, a process that is strongly dependent on the field strength. Sun and Stafström [5] have used the SSH model to investigate the formation of excited states through the recombination process between two oppositely charged polarons in a system composed of two coupled conjugated polymer chains. In this case it is reported that, depending on the interchain distance and the electric

field strength, the two polarons can either recombine into an exciton, become bound together forming a polaron pair or pass each other. Furthermore, it was found that the singlet states are always easier to be formed than the triplet ones. These facts indicate that in PLEDs, the electroluminescence quantum efficiency can exceed the statistical limitation value of 25%. Very recently, our previous research has shown that the presence of impurities in a conjugated polymer lattice, for several electric field regimes, favors the excited states formation thus improving the excitation yields when the scattering between oppositely charged polarons is considered [9]. There are, however, still many controversial aspects regarding the influence of some physical process such as temperature, electric field strength, coulomb interactions, and impurity effects on the formation of excited states via recombination process between oppositely charged carriers, which requires detailed phenomenological descriptions. Of particular importance is the determination of critical values of temperature and electric field in terms of the resulting products of collisions between quasi-particles.

In this paper, a systematic numerical investigation considering the influence of thermal effects, an external electric field and Coulomb interactions on the formation of excited states via recombination processes between an oppositely charged polaron pair is performed using a cis-polyacetylene chain in the framework of a nonadiabatic evolution method. An Ehrenfest Molecular Dynamics is performed by using a one-dimensional tight-binding model including lattice relaxation. Combined with the Extended Hubbard Model (EHM), a modified version of the SSH model is used to include the Brazoviskii-Kirova symmetry breaking term. Temperature effects are included by means of a canonical Langevin equation. The aim of this work is to give a physical picture of the products derived from the recombination of oppositely charged polarons in conjugated polymers, when temperature effects are considered, and contribute to the understanding of these important processes, that may provide guidance for improve electroluminescence yields in PLDEs.

II. MODEL AND METHOD

A cis-polyacetylene chain is used to study the recombination process of two oppositely charged polarons in conjugated polymers. The overall Hamiltonian is given by $H = H_{SSH} + H_{ee}$. The first term is the SSH-type Hamiltonian [12, 13] modified to include an external

electric field and the Brazovskii-Kirova symmetry-breaking [14], that has the following form:

$$H_{SSH} = -\sum_{n,s}\left(t_{n,n+1}C^{\dagger}_{n+1,s}C_{n,s} + h.c.\right) + \sum_{n}\frac{K}{2}y_n^2 + \sum_{n}\frac{p_n^2}{2M}, \quad (1)$$

where n indexes the sites of the chain. The operator $C^{\dagger}_{n,s}$ ($C_{n,s}$) creates (annihilates) a π-electron state at the nth site with spin s; K is the harmonic constant that describes a σ bond and M is the mass of a CH group. The parameter y_n is defined as $y_n \equiv u_{n+1} - u_n$, where u_n is the lattice displacement of an atom at the nth site. p_n is the conjugated momentum to u_n and $t_{n,n+1}$ is the hopping integral [15], given by $t_{n,n+1} = e^{-i\gamma A(t)}\left[(1+(-1)^n\delta_0)\,t_0 - \alpha y_n\right]$, where t_0 is the hopping integral of a π-electron between nearest neighbour sites in the undimerized chain, α is the electron-phonon coupling, and δ_0 is the Brazovskii-Kirova symmetry-breaking term, which is used to take the cis-symmetry of the polymer into account. $\gamma \equiv ea/(\hbar c)$, with e being the absolute value of the electronic charge, a is the lattice constant, and c is the speed of light. The relation between the time-dependent vector potential $\mathbf{A}$ and the uniform electric field $\mathbf{E}$ is given by $\mathbf{E} = -(1/c)\dot{\mathbf{A}}$ [16].

The last contribution denotes e-e interactions and can be written as

$$H_{ee} = U\sum_{i}\left(C^{\dagger}_{i,\uparrow}C_{i,\uparrow} - \frac{1}{2}\right)\left(C^{\dagger}_{i,\downarrow}C_{i,\downarrow} - \frac{1}{2}\right) + V\sum_{i}\left(n_i - 1\right)\left(n_{i+1} - 1\right), \quad (2)$$

where U and V are the on-site and nearest-neighbor Coulomb repulsion strengths, respectively, and $n_i = C^{\dagger}_{i,\uparrow}C_{i,\uparrow} + C^{\dagger}_{i,\downarrow}C_{i,\downarrow}$ [17]. It should be noted that the inclusion of the additional constant factors (related to the conventional description of the Hubbard model) is necessary in order to maintain the electron hole symmetry of the Hamiltonian. The many-body problem is treated using the unrestricted Hartree-Fock (UHF) approximation. The single determinant considered in this formalism is built through the use of a number of single-particle orbitals, which are optimized according to the variational principle. A modified version of the SSH model that includes Coulomb interactions using an UHF approach can capture the essential electronic properties of quasi-particles transport in conjugated polymers, and has been successfully applied in many relevant studies of the field for over three decades [5, 18, 19]. The parameters used here are $t_0 = 2.5\ eV$, $M = 1349.14\ eV \times fs^2/\text{Å}^2$, $K = 21\ eV\text{Å}^{-2}$, $\delta_0 = 0.05$, $\alpha = 4.1\ eV\text{Å}^{-1}$, $a = 1.22$ Å, and a bare optical phonon energy $\hbar\omega_Q = \hbar\sqrt{4K/M} = 0.16\ eV$. These values have been used in previous simulations and are expected to be valid for conjugated polymers in general [20–26].

In order to solve these equations numerically, first a stationary state that is self-consistent with all degrees of freedom of the system (lattice and electrons) is obtained. The initial bond configuration and the electronic structure of a polymer chain containing a hole-polaron and an electron-polaron can be obtained by solving the following self-consistent equations of the bond configuration $\{u_n\}$ and the electronic wave functions $\{\phi_n\}$:

$$u_{n-1} - u_n = -\frac{2\alpha}{K}\sum_{\mu}\phi_\mu(n)\phi_\mu(n+1) + \frac{2\alpha}{NK}\sum_{\mu,n}\phi_\mu(n)\phi_\mu(n+1), \tag{3}$$

$$\varepsilon_\mu\phi_\mu(n) = -[t_0 - \alpha(u_{n-1} - u_n)]\phi_\mu(n+1) - [t_0 - \alpha(u_n - u_{n-1})]\phi_\mu(n-1) \tag{4}$$

where ε_μ is the eigenvalue of μ-th energy level. We begin by constructing the Hamiltonian from a $\{y_n\}$ set of positions that is a composition of two isolated polarons. By solving the time-independent Scrhödinger equation, a new set of coordinates $\{y'_n\}$ is obtained. Iterative repetitions of this procedure yields a self-consistent initial state when $\{y_n\}$ is close enough to the solution. The equation of motion that describes the site displacement and provides the temporal evolution of the lattice is obtained by a classical approach. The nuclear dynamics is carried out with the Euler-Lagrange equations

$$\frac{d}{dt}\left(\frac{\partial\langle L\rangle}{\partial\dot{u}_n}\right) - \frac{\partial\langle L\rangle}{\partial u_n} = 0, \tag{5}$$

where $\langle L\rangle = \langle T\rangle - \langle V\rangle$. Eq. 5 leads to a newtonian equation $M\ddot{u}_n = F_n(t)$. Thus,

$$\begin{aligned} F_n(t) = M\ddot{u}_n(t) = &-K\left[2u_n(t) - u_{n+1}(t) - u_{n-1}(t)\right] \\ &+ \alpha\left[B_{n,n+1}(t) - B_{n-1,n}(t) + B_{n+1,n}(t) - B_{n,n-1}(t)\right], \end{aligned} \tag{6}$$

where, $F_n(t)$ represents the force on the nth site [27]. Here, $B_{n,n'}(t) = \sum_{k,s}{}'\psi^*_{k,s}(n,t)\,\psi_{k,s}(n',t)$ is the term that couples the electronic and lattice solutions. The primed summation represents a sum over occupied states.

The time dependent wave functions are constructed by means of a linear combination of instantaneous eigenstates of the electronic Hamiltonian. The solutions of the time-dependent Schrödinger equation can be put in the form

$$\psi_{k,s}(n,t_{j+1}) = \sum_l\left[\sum_m \phi^*_{l,s}(m,t_j)\,\psi_{k,s}(m,t_j)\right]\times e^{(-i\varepsilon_l\Delta t/\hbar)}\phi_{l,s}(n,t_j). \tag{7}$$

$\{\phi_l(n)\}$ and $\{\varepsilon_l\}$ are the eigenfunctions and the eigenvalues of the electronic part for the Hamiltonian (within the Unrestricted Hartree-Fock approximation) at a given time t_j [28].

Equation (6), which governs the evolution of the lattice system, can be numerically integrated using the method

$$u_n(t_{j+1}) = u_n(t_j) + \dot{u}_n(t_j)\Delta t, \tag{8}$$

$$\dot{u}_n(t_{j+1}) = \dot{u}_n(t_j) + \frac{F_n(t_j)}{M}\Delta t. \tag{9}$$

Hence, the electronic wave functions and the lattice displacements at the $(j+1)$th time step are obtained from the jth time step. At time t_j the wave functions $\{\psi_{k,s}(i,t_j)\}$ is expressed as an expansion of the eigenfunctions $\{\phi_{l,s}\}$ at that moment: $\psi_{k,s}(i,t_j) = \sum_{l=1}^{N} C^s_{l,k}\phi_{l,s}(i)$, where $C^s_{l,k}$ are the expansion coefficients. The occupation number for each eigenstate $\phi_{l,s}$ is $\eta_{l,s}(t_j) = \sum_k{}'|C^s_{l,k}(t_j)|^2$. $\eta_{l,s}(t_j)$ contains information concerning the redistribution of electrons among the energy levels [9].

Here, the temperature effects are simulated by adding thermal gaussian random forces with zero mean value $\langle\zeta_n(t)\rangle \equiv 0$ and variance $\langle\zeta_n(t)\zeta_n(t')\rangle = 2k_BT\gamma M\delta(t-t')$. We adopted a white stochastic signal $\zeta_n(t)$ as the fluctuation term. Also, in order to keep the temperature constant at its initial value after a transient period (named thermalization), it is necessary to introduce a damping factor, γ. Therefore, Eq. (6) is modified to $M\ddot{u} = -\gamma\dot{u} + \zeta_n(t) + F_n(t)$. The modified Eq. 4 no longer defines a set of ordinary differential equations (ODEs); rather, in this formalism we deal with a set of stochastical differential equations (SDEs). It is then important to find a proper integrator for solving SDEs. Since our model assumes a classical treatment for the lattice, it is possible to use the regular Langevin-type approach to take thermal effects into account. Various discretizations of the modified Eq. (6) are available in the literature. We have used the velocity-verlet (Eqs. 6 and 7) that is very similar to the popular BBK integrator [29]. Furthermore, we have introduced both the dissipative force and the gaussian random force in such a way to possess the power spectral density given by the fluctuation-dissipation theorem. In this way, the fluctuations can be obtained by using

$$\zeta_n(t) = \sqrt{(2k_BT\gamma M)/\Delta t} \times Z^n, \tag{10}$$

where Z^n is a random number. The damping constant can be determined by low temperature lattice thermal conductivity measurements. The γ value used here has the same order of magnitude as expected from experimental data of Raman spectral line width in polydiacetylene (γ=$0.01\omega_Q$) [30]. It should be emphasized that this procedure of including temperature effects by means of a Langevin formalism has been extensively used in the literature and is known to yield excellent qualitative results [31–37].

III. RESULTS

A systematic numerical investigation concerning the influence of temperature effects, an external electric field, and Coulomb interactions over the recombination dynamics of two oppositely charged polarons is performed in systems composed of 200-site cis-polyacetylene chains with periodic boundary conditions. For the electric field, turned on quasi-adiabatically [32], the values used in the simulations varied from 0.1 to 2.0 mV/Å with an increment of 0.1 mV/Å, whereas the temperature regimes considered ranged from 0 to 200 K with a step of 10 K. For the on-site electron-electron interactions the value considered is $U = 0.2t_0$. The nearest-neighbor Coulomb repulsion strength is determined by using the relation V = U/2. It is worthy to mention that, although some relevant studies have reported results using U levels higher than 4.0 eV [34, 38], recently a considerable amount of studies has been performed considering moderated values of electron-electron interactions in a range of 0.5-3.0 eV [3, 5, 7–9, 11, 18, 19, 39–44]. In this context, Figure 1 presents the schematic diagram of energy levels for a lattice containing a hole-polaron (positive carrier) and an electron-polaron (negative carrier). These charge carriers are formed removing or adding electrons to the polymer chain, causing lattice distortions and the rising of energy levels to the inside of the band gap. A single polymer chain containing a hole-polaron, is represented by the absence of one electron in the HOMO level and the absence of two electrons in the LUMO+1 level, which yields a +1e charge. On the other hand, an electron-polaron is represented by the levels HOMO-1 and LUMO, in which the upper one is occupied by one electron and the lower one occupied by two electrons, yielding a -1e charge.

The discussion concerning the products of the collision process between oppositely charge carriers starts by the analysis of the polaron-polaron interaction under a temperature regime of 50 K and an electric field strength of 1.5 mV/Å, as shown in Figure 2. The temporal evolution of the staggered bond-length, $\bar{y}(t) = (-1)^n[y_{n-1}(t) + 2y_n(t) + y_{n+1}(t)]/4$, depicts the dynamical process. An excited state is formed directly after the collision between the polaron pair, as presented in Figure 2(a) (channel 1). Initially, the electron-polaron is located at the 60th site while the hole-polaron is at 150th site. The two charge carriers are separated far enough from each other so that they behave as independent structures. After a small transient time for the electric field response, the polarons begin to move towards one another due to the different charges. The polaron dynamics before the collisional processes occurs

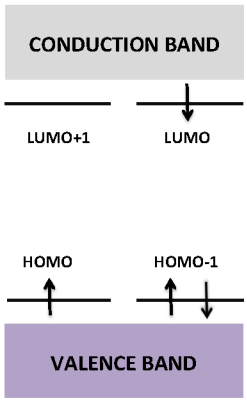

FIG. 1: The schematic diagram of energy levels for a polymer chain containing an electron-polaron and a hole-polaron.

as already described in the literature [33, 37]. At approximately 150 fs, when the collision takes place, one can see that the electron-polaron and the hole-polaron recombines into a well defined lattice structure from the lattice distortion point of view. This process, however, yields the formation of only one neutral excited state after the collision. Furthermore, it can be seen that after about 50 fs, the adding up of thermal energy begins to become visible through the blurring of the figure (cyan regions). The interaction between the two original polarons produces phonons after the collision that, combined with the thermal oscillations, generates even more energetic phonons represented mainly by the dark blue regions closer to the site where the collision has occurred, as shown in Figure 2(a). Another important aspect that can be noted in this figure is obtained by comparing the lattice deformation of the excited state generated after the collision with the lattice defect that characterizes any of the polarons at the beginning of the simulation. The lattice distortion for the exciton is wider than that of the polarons, which shows that the distortion for neutral excitations involve a higher number of sites. Also, the red and yellow regions, not present in the polarons lattice defects, indicates a higher level in deformation of the lattice, which suggests that excitons are more stable structures than polarons [5].

Figure 2(b) depicts the temporal evolution of mean charge density $\bar{\rho}(t) = 1 - [\rho_{n-1}(t) + 2\rho_n(t) + \rho_{n+1}(t)]/4$ for the polaron pair collision in this first channel — the recombination process reported so far. Immediately after their encounter, the charges of the two polarons cancel each other. It can be conjectured that the charge cancelation process occurs due to

excited state formation. Also, it is possible to note small charge density fluctuations associated with the localized excitation, where the positive and negative charges are bounded together. Indeed, the charge density alternates across the lattice deformation for the localized excited stated, creating an oscillating molecular electric dipole. Recently, Silva and coworkers reported a similar behavior where a neutral soliton showed an infrared signature that comes from a temperature-induced electric dipole on the lattice deformation of that well-localized excitation [36]. This fact may suggests that the oscillating electric dipoles induced by temperature effects are some sort of general feature when neutral excitations are considered. It is important to note that this channel of polaron pair recombining into a neutral structure is only observed for electric fields strengths between 0.8–1.5 mV/Å and temperature regimes of 50–160 K. It is due to the fact that the temperature damps the polarons motion avoiding the interaction between them [33]. Furthermore, the simulation presented in Fig. 2(b) yield a neutral excited state with a better rate than those previously reported by An and colleagues [4], where exactly the same kind of calculations were performed in the absence of Coulomb interactions and temperature effects. In An's studies, for the a electric field strength of 1.2 mV/Å, it was observed an inelastic scattering processes between oppositely charged polarons into an mixed state composed of polarons and excitons. The lattice fluctuations and the high energy of phonons provided by the inclusion of thermal effects, absent in An's work, are responsible for this better yield of neutral excitations.

The temperature influence over the collisional process of the charge carriers can be better considered by a thermal bath with temperature four times higher as the one considered in channel 1 and also an electric field strength of 1.5 mV/Å, as shown in Fig. 3 (channel 2). For the sake of conciseness we chose to present only the results of mean charge density evolution, for these are more instructive than the bond length evolution. In this case it can be seen that the electron-polaron is annihilated immediately after the collision, whereas the hole-polaron is not completely dissociated before 600 fs. This channel gives rise to a final state where a dimerized lattice is obtained. The effects of the temperature increasing can be readily noted by comparing the diffusive pattern presented by the charge concentration of the charge carriers to that of Fig 2(b). Also, the lattice oscillations imposed by the random forces are of such amplitudes that the polarons have reduced stability. The charge delocalization presented in Fig. 3 is the typical signature of the absence of the polaron structure in the system, which leads to a dimerized lattice. These results show that there

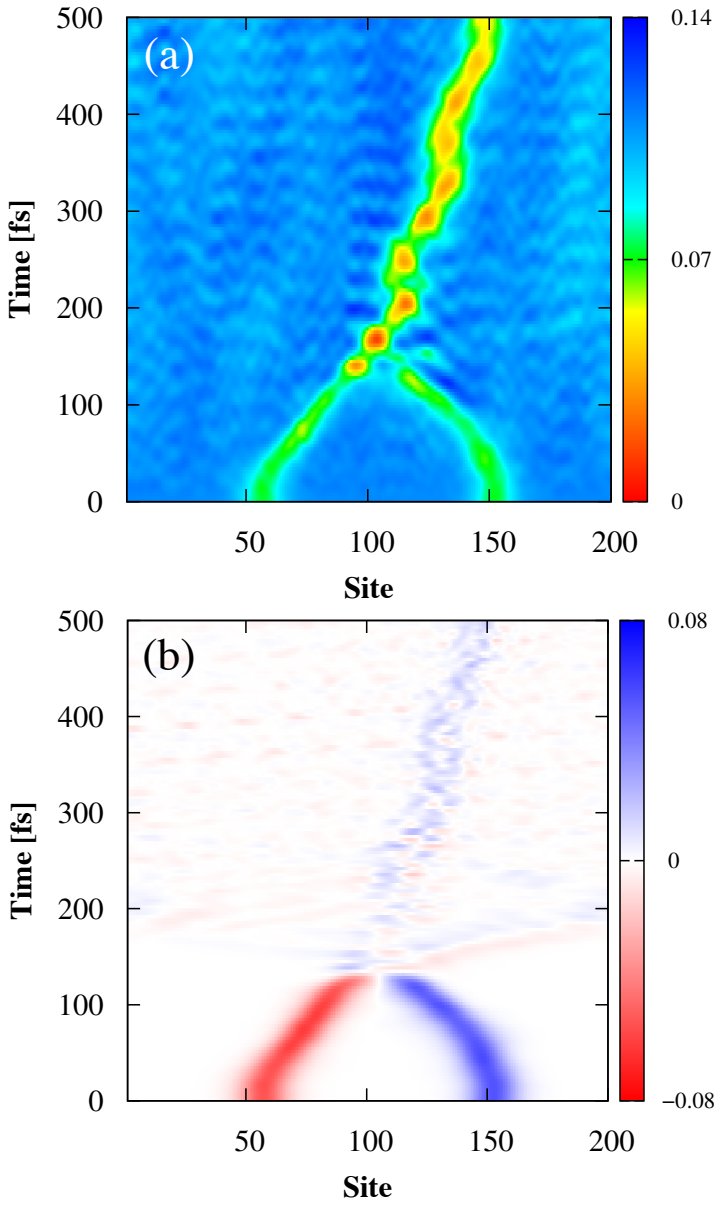

FIG. 2: (a) Staggered bond-length and (b) mean charge density time evolution for an electric field strength of 1.5 mV/Å and temperature regime of 50 K.

are different products formed after the collisional process depending on temperatures and electric field strength. On one hand this is consistent with the critical electric field strength reported recently by An and collaborators for the formation of a polaron-exciton structure[4], but on the other hand the more realistic description we have made resulted in different values from the quantitative point of view. Our results points towards a critical field strength of 1.5

mV/Å where only neutral excitations are formed. Indeed, the markedly different behavior is caused by the temperature influence over the system, a kind of effect absent in the work of An [4]. The lattice vibrations damps the charge carrier motion for electric field strengths smaller than 1.5 mV/Å, as already discussed, resulting in a transition for the quasi-particle dynamics from a drift driven by the electric field to a random walk dynamics imposed by the random forces. This can be responsible for the differences in the final products obtained here. In this way, we believe that an approach that takes into account thermal effects over the charge carrier collision is crucial for the correct description of more realistic polymers, that are suitable for actual technologic applications.

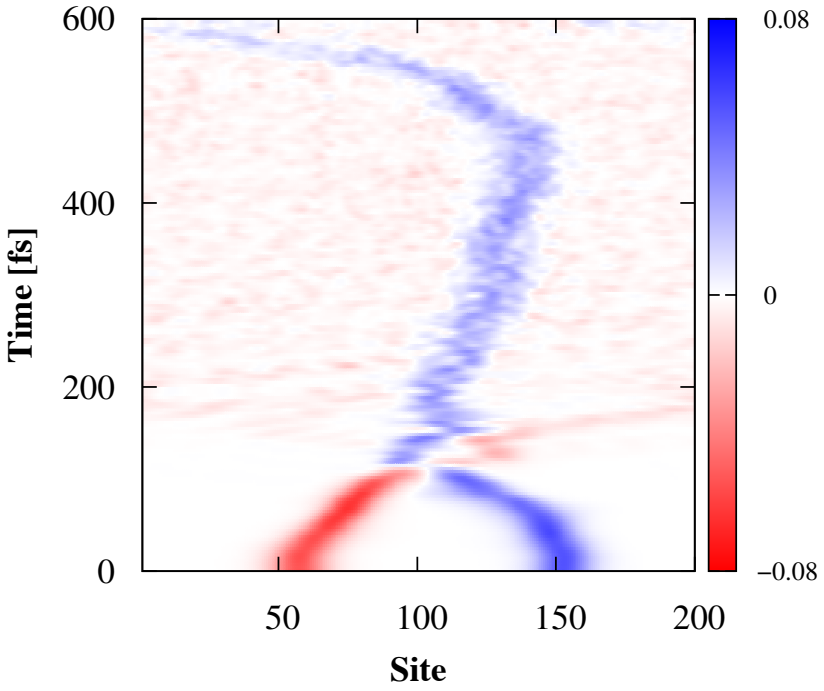

FIG. 3: Mean charge density time evolution for an electric field strength of 1.5 mV/Å and temperature regime of 200 K.

The previous discussion on the creation of neutral excited states is confirmed by an analysis of the occupation number presented in Figure 4. Note that this figure shows the time evolution of the occupation numbers for the intra-gap levels related to Fig. 1. Initially, there are four levels inside the band gap, which are localized electron states corresponding to the two lattice defects. At the beginning of the process (first few 100 fs) these energy levels are degenerated because the two polarons are initially far apart. During this transient regime,

the occupation number of the LUMO level sharply decreases from 1 to 0; simultaneously, the occupation number of LUMO+1 sharply increases from 0 to 1. This change in occupation number reflects the fact that these two levels interchange positions, a process that is energetically accessible due to the degeneracy. The electron transfer associated with this change is mostly due to the fact that the wavefunction corresponding to this level is spreaded over the whole chain. This process occurs in a similar fashion between HOMO-1 and HOMO levels. Once again, these changes do not correspond to the transfer of an electron from one level to another; instead, they occur as a result of changes in the eigenenergies of the respective levels. After 200 fs, the degeneracy is broken by the interplay between electric field and the electron-electron interactions and by the coupling between the two polarons when they are close to each other. From that moment on, the interchange between the positions of the energy levels is no longer observed. Very recently, a similar behavior for abrupt changes on the occupation number was reported by Sun and Stafström [34]. Considering channel 1 (black lines in Fig. 4), before the transient period in which the occupation number oscillates due to the collision, it is possible to note that the final state in LUMO+1 level is not covered by an integer number, which is evidence of partial electron transfer from the LUMO level. Since the LUMO level stays completely empty after 300 fs the remaining fraction of this level, which was not transferred to LUMO+1, decays to the HOMO level resulting in an photon emission process. Similar to the occupation process for the LUMO+1, the HOMO level receive the electron fraction transferred from the HOMO-1, while the occupation of the HOMO-1 level remains unchanged after the partial transfer. For channel 2 (red lines in Fig. 4), after 600 fs the occupation number for the LUMO level drops to zero (a photon emission process) which indicates the complete annihilation of the polaron, whereas the HOMO level is fully occupied by two electrons. Both HOMO-1 and HOMO levels are occupied by two electrons after 600 fs; on the other hand the LUMO and LUMO+1 levels become empty. This final configuration for the occupation numbers reported in channel 2, results in a dimerized lattice where the polaron defect an absent. In this way, these results indicate that, in general, the combination of the mechanisms of partial electron transfer among the levels together with a photon emission will induce the formation of neutral states only for low temperature regimes (below 150 K). Whenever the temperature is higher than this critical value a dimerized lattice is observed to take place.

While the occupation number analysis is the most suitable tool in studying the process

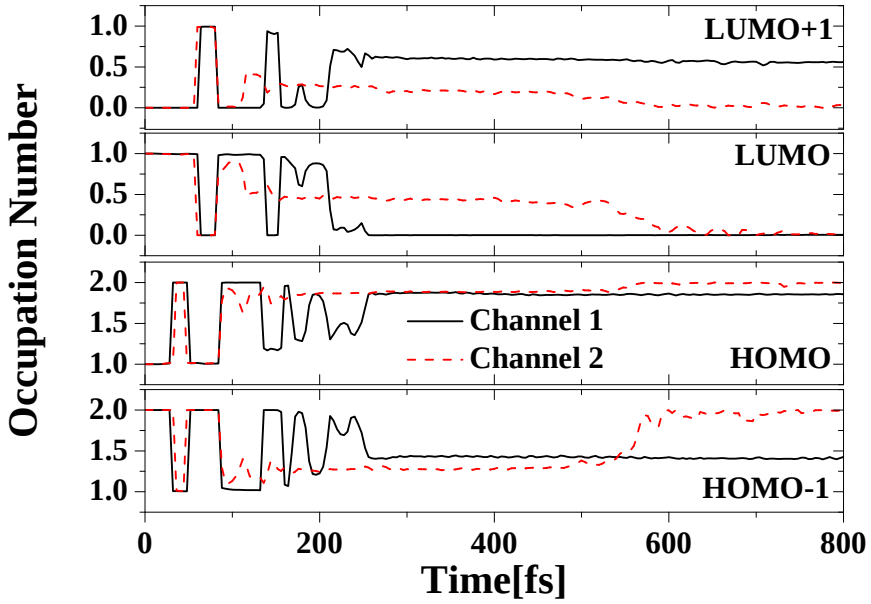

FIG. 4: Time evolution of the occupation number of the intra-gap energy levels, where the black lines represents channel 1 (50 K and 1.5 mV/Å) and the red lines depicts channel 2 (200 K and 2.0 mV/Å).

the leads to the formation of new species such as excited states, the stability of the quasi-particles is better described by means of the energy levels time evolution. We finish our discussion by presenting in Figure 5 the time evolution profile of the intra-gap energy levels of the simulations shown in Figs. 2 and 3. As can be seem from Fig. 5, at the beginning of the simulation there are four intra-gap levels, which are electron states caused by the presence of the polarons in the lattice. Fig. 5(a) depicts the process discussed in channel 1, where an exciton is formed directly. At about 50 fs, the degenerate levels rapidly become nondegenerated due to the temperature influence and the electron-electron interactions. The collisional process between the two polarons is noted to take place at about 200 fs, when the resulting phonons are associated to the slightly deeper oscillations of the energy levels inside the band gap. As both polarons are annihilated and one exciton arises after the interaction between the charge carriers, one can see that the two intra-gap levels HOMO-1 and LUMO+1 return to the valence and conduction bands, respectively. On the other hand, the HOMO and LUMO levels remain inside the band gap until the end of the simulation, presenting a new configuration that is located deeper inside the gap than at the beginning. According to their wave functions, we know that the exciton energy levels present a larger

narrowing than those of polarons. This suggests that excitons are structures more stable than polarons. Regarding the process discussed in channel 2, the signature of the loss of stability of the polarons, that leads to a dimerized, lattice is related to the LUMO's and HOMO's levels returning to the conducting and valence bands, respectively, as shown in Fig. 5(b). Furthermore, the oscillations presented by the energy levels are resulting from the motion of the sites of the lattice influenced by the thermal random forces, as can be seen in Fig. 5(a) and (b).

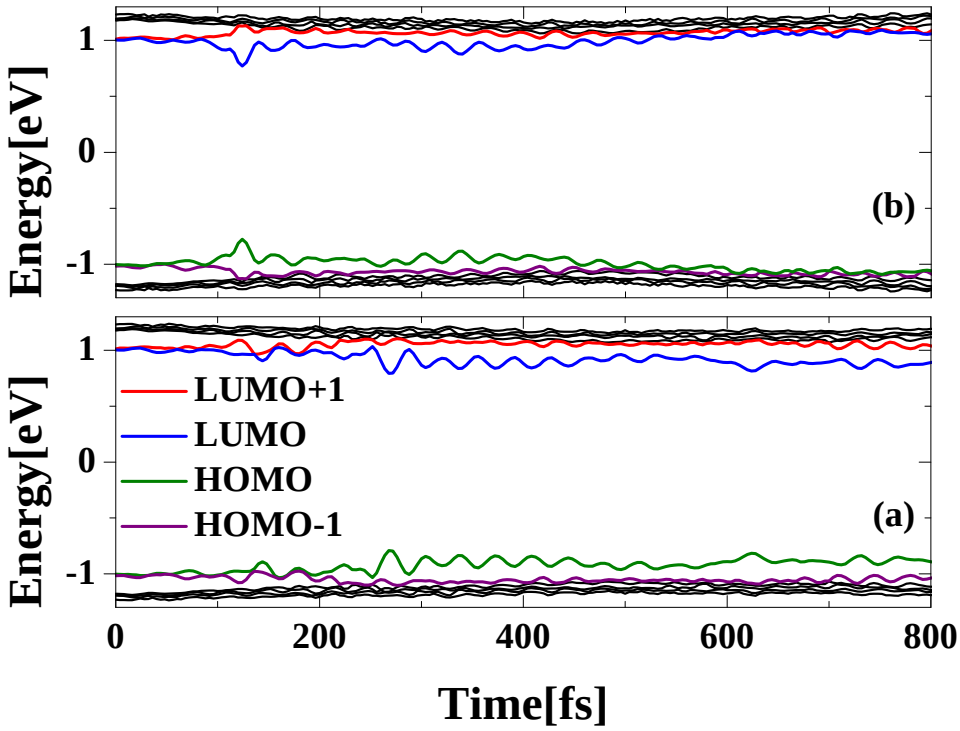

FIG. 5: Time evolution of the energy levels for (a) channel 1 - 50 K and (b) channel 2 - 200 K considering an electric field strength of 1.5 mV/Å.

As discussed above, the polaron–polaron reaction induces electron redistribution among levels, i.e., there are other different electronic states after the collisional process between these charge carriers. As showed in Figs. 4 and 5, we found that there are mainly two new electronic states after collision, when temperature effects are taken into account, which are shown in Fig. 6. However, a third electronic state (named polaron-exciton) can occur after a reactive scattering between an oppositely charged polaron-pair as mentioned above and reported in recent works [3, 4, 6, 9–11]. Here, the state (a) denotes the initial electron

distribution, represented in Fig. 1, which contains an oppositely charged polaron–pair. State (b) denotes the final electronic configuration after the formation of an neutral excited state (channel 1). The dimerized lattice, channel 2, is represented in the state (c). Finally, state (d) denotes the intra-gap configuration for a system that contains two polaron-excitons.

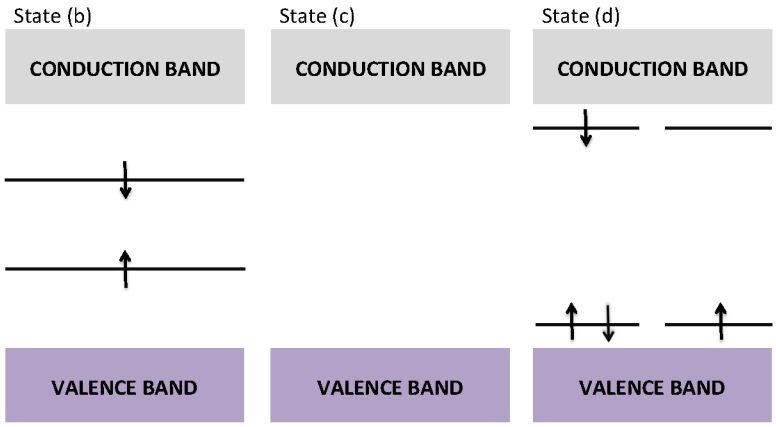

FIG. 6: The schematic diagram of energy levels for a polymer chain (b) containing a neutral excitation, (c) considering a pristine lattice, and (d) containing two oppositely charged polaron-excitons.

We now discuss the yields for these states using a projection method [18]. After each evolution step, the lattice displacements $\{u_n\}$ are determined, and the Hartree-Fock Hamiltonian of the system is also obtained. One can, then, obtain all single electron eigen wavefunctions $\{\phi_i\}$ by diagonalizing the Hamiltonian matrix. Any desired eigenstate of the system can thus be constructed using these single electron wavefunctions in the form of a Slater determinant, $|\Phi_k\rangle = |\phi_{1\downarrow}\phi_{1\uparrow}\phi_{2\downarrow}\phi_{2\uparrow}...\rangle$. For example, the ground-state involves all single electron states in the valence band. Here, the desired eigenstate is the neutral excited state. The yield of the eigenstates $|\Phi_k\rangle$ is obtained by projecting it on the evolutional wave function $|\Psi(t)\rangle$ which is also a Slater determinant constructed of single electron evolutional wave functions $\{\psi_j(t)\}$, $|\Psi_k\rangle = |\psi_{1\downarrow}\psi_{1\uparrow}\psi_{2\downarrow}\psi_{2\uparrow}...\rangle$, i. e., $I_K = |\langle\Phi_k|\Psi(t)\rangle|^2$ [45, 46]. Fig. 7 shows the time dependence of the yields for states (a) and (b) during the polaron-polaron interaction. It can be seen that the yield of state (a) remains at 100% before 80 fs. This fact denotes that the polarons does not interact during this period. From 80 to 200 fs, the yield of state (a) drops about 30% whereas state (b) rises approximately 70 %, with some fluctuations that are resulting of the collisional process. This suggests that, in this regime,

these states are mixed. After 300 fs, the yield of state (a) sharply drops to zero. At the same time, the yield of state (b) increase to about 95%. This explicitly shows that state (b) is mostly the unique state after the collision. As previously discussed, state (b) (channel 1) contains a neutral excited state. The remaining yield of the state (a), which was not converted into the state (b) ($\sim 5\%$), denotes a free carrier, i. e., the polaron-polaron interaction may transfer electrons from the intra-gap energy levels to the conduction band with some probability after collision. Thus, the results indicate that an excited neutral state and a free carrier can be produced by the polaron-polaron reaction.

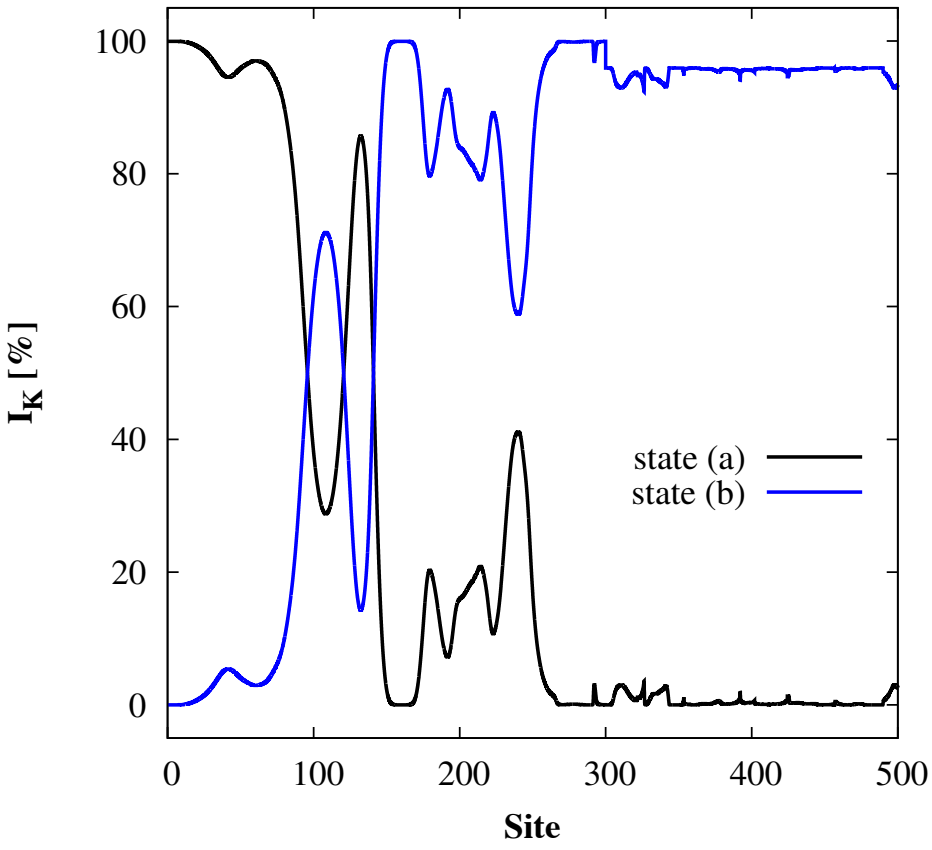

FIG. 7: Time dependence of the yields for states (a) and (b) which are shown in Figs. 1 and 6, respectively.

We have calculated the yields of state (a) for different electric field and temperature regimes. The results are displayed in Fig. 8. The blue region denotes the regimes where the interplay between the electric field and temperature is not favorable to the formation of neutral excited states, i. e., the yield values are zero. Below the critical electric field strength

of 0.8 mV/Å and for temperature regimes smaller than 50 K, the interplay between these two effects favors the polaron-exciton formation (state (d)) in the same way as reported in the references [3, 4]. If the temperature lies in the regime 50-200 K, the polaron motion is damped and the reaction between them is no longer observed. However, just above the critical electric field strength, about 1.5 mV/Å, the yield of state (a) sharply increases to about 60-95%, considering a temperature regime that lies in 50-160 K regime. It shows that the electric field strength dominates the motion of the polarons over the random motion imposed by the thermal effects. The abrupt change in the yield values of the specie formed after the interaction between the oppositely charged carriers is recognized as a standard behavior of this process [3, 18, 47]. Considering electric field strengths higher than 1.5 mV/Å, the collision process annihilates the polarons producing a final state (state (c)) where a dimerized lattice is obtained. Also, the lattice oscillations imposed by the random forces are of such amplitudes that the polarons have reduced stability, as mentioned before. Considering temperatures higher than 200 K, the interplay between electric field and temperature annihilates the polaron, even before the collision process, as reported in the reference [33].

IV. CONCLUSIONS

In summary, using a tight-binding electron-phonon interaction model modified to include an external electric field, electron-electron interactions, and temperature effects the recombination processes between an electron-polaron and a hole-polaron has been simulated in a conjugated polymer lattice, by means of nonadiabatic molecular dynamics. The results show that there are two channels resulting from the recombination between the polarons: channel 1, where a critical temperature regime exists, below which a neutral excitation is directly formed channel 2, where a dimerized lattice is the resulting product of the collisional process for temperatures higher than the critical value. Furthermore, it is found that both channels depend sensitively on the strength of the applied electric field. These significant results reveal remarkable details concerning the polaron recombination reaction and provide guidance to understanding electroluminescence processes in Polymer Light Emitting Diodes.

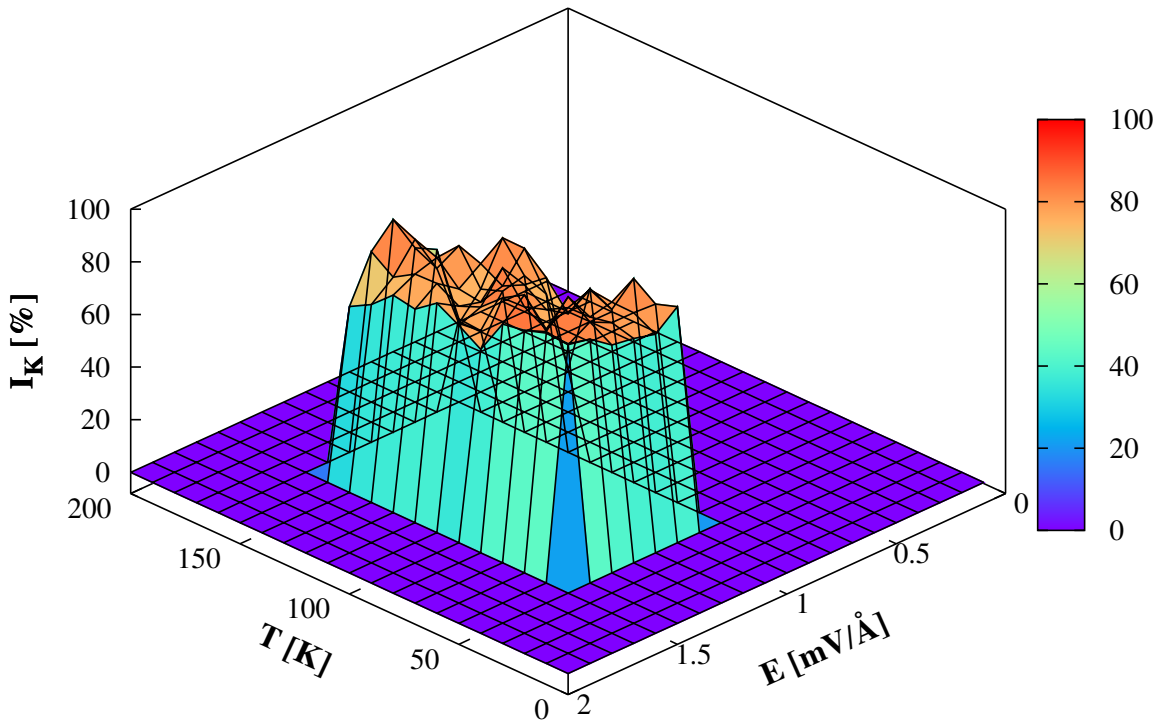

FIG. 8: Final yield values for state (a) after 1 ps as a function of the electric field strength and temperature effects.

Acknowledgements

The authors gratefully acknowledge the Swedish Research Council (VR) for financial support, the Swedish National Infrastructure for Computing (SNIC), and the and the financial support from the Brazilian Research Councils CNPq, CAPES and FINATEC.

[1] A. E. Jailaubekov, A. P. Willard, J. R. Tritsch, W.-L. Chan, N. Sai, R. Gearba, L. G. Kaake, K. J. Williams, K. Leung, P. J. Rossk, et al., Nat. Mat. **12**, 66 (2013).

[2] M. S. White, M. Kaltenbrunner, E. D. Gowacki, K. Gutnichenko, G. Kettlgruber, I. Graz, S. Aazou, C. Ulbricht, D. A. M. Egbe, M. C. Miron, et al., Nat. Phot. **7**, 811 (2013).

[3] J. Lei, Z. Sun, Y. Zhang, and S. Xie, Org. Elec. **10**, 1489 (2011).

[4] Z. An, B. Di, and C. Q. Wu, Eur. Phys. J. B. **63**, 71 (2008).

[5] Z. Sun and S. Stafström, J. Chem. Phys. **135**, 074902 (2011).

[6] Z. Sun and S. Stafstöm, J. Chem. Phys. **136**, 244901 (2012).

[7] B. Di, Y. Meng, Y. D. Wang, X. J. Liu, and Z. An, J. Chem. Phys. B. **115**, 964 (2011).

[8] B. Di, Y. Meng, Y. D. Wang, X. J. Liu, and Z. An, J. Chem. Phys. B. **115**, 9339 (2011).

[9] L. A. Ribeiro, W. F. da Cunha, P. H. O. Neto, R. Gargano, and G. M. e Silva, J. Chem. Phys. **139**, 174903 (2013).

[10] Q. Lu, H. Zhao, Y. Chen, and Y. Yan, Physica B **412**, 13 (2013).

[11] Y. Li, K. Gao, Z. Sun, S. Yin, D. sheng Liu, and S. jie Xie, Phys. Rev. B. **78**, 014304 (2008).

[12] W. P. Su, J. R. Schrieffer, and A. J. Heeger, Phys. Rev. Lett. **42**, 1698 (1979).

[13] W. P. Su, J. R. Schrieffer, and A. J. Heeger, Phys. Rev. B. **22**, 2099 (1980).

[14] S. Brazovskii and N. Kirova, Chem. Soc. Rev. **39**, 2453 (2010).

[15] C. S. Pinheiro and G. M. e Silva, Phys. Rev. B. **65**, 094304 (2002).

[16] S. Stafström, Chem. Soc. Rev. **39**, 2484 (2010).

[17] Z. G. Yu, M. W. Wu, X. S. Rao, and A. R. Bishop, J. Phys. Condes. Matter **8**, 8847 (1996).

[18] Z. Sun, Y.Li, K. Gao, D. Liu, Z.An, and S. Xie, Org. Elec. **11**, 279 (2010).

[19] Z. Sun and S. Stafstöm, J. Chem. Phys. **134**, 044906 (2011).

[20] P. H. O. Neto, W. F. da Cunha, J. F. Teixeira, R. Gargano, and G. M. e Silva, J. Phys. Chem. Lett **3**, 3039 (2012).

[21] L. A. Ribeiro, W. F. da Cunha, P. H. O. Neto, R. Gargano, and G. M. e Silva, Chem. Phys. Lett. **555**, 168 (2013).

[22] L. A. Ribeiro, W. F. da Cunha, P. H. O. Neto, and G. M. e Silva, Phys. Proc. **28**, 112 (2012).

[23] A. Johansson and S. Stafström, Phys. Rev. Lett. **86**, 3602 (2001).

[24] A. Johansson and S. Stafström, Phys. Rev. B. **69**, 235205 (2004).

[25] Z. An, C. Q. Wu, and X. Sun, Phys. Rev. Lett. **93**, 216407 (2004).

[26] G. M. e Silva and A. Terai, Phys. Rev. B. **47**, 12568 (1993).

[27] G. M. e Silva, Phys. Rev. B. **61**, 10777 (2000).

[28] M. P. Lima and G. M. e Silva, Phys. Rev. B. **74**, 224303 (2006).

[29] J. M. W. R. D. S. J. A. Izaguaire, D. P. Catarello, J. Chem. Phys. **114**, 2090 (2001).

[30] G. Cerullo, G. Lanzani, M. Z. S. S. de Silvestri, S. D. Comoretto, I. Moggio, and G. Dellepiane, Synth. Met. **116**, 57 (2001).

[31] L. A. Ribeiro, P. H. O. Neto, W. F. da Cunha, L. F. Roncaratti, R. Gargano, D. A. da Silva Filho, and G. M. e Silva, J. Chem. Phys. **135**, 224901 (2011).

[32] L. A. Ribeiro, W. F. da Cunha, P. H. O. Neto, R. Gargano, and G. M. e Silva, Chem. Phys. Lett. **580**, 108 (2013).

[33] L. A. Ribeiro, W. F. da Cunha, P. H. O. Neto, R. Gargano, and G. M. e Silva, New J. Chem. **37**, 2829 (2013).

[34] Z. Sun and S. Stafström, J. Chem. Phys. **138**, 164905 (2013).

[35] P. H. O. Neto, W. F. da Cunha, L. F. Roncaratti, R. Gargano, and G. M. e Silva, Chem. Phys. Lett **493**, 283 (2010).

[36] L. F. Roncaratti, R. Gargano, P. H. de Oliveira Neto, W. F. da Cunha, D. A. da Silva Filho, and . G. M. e Silva, Chem. Phys. Lett. **593**, 214 (2012).

[37] L. F. Roncaratti, R. Gargano, and G. M. e Silva, J. Phys. Chem. A. **113**, 14591 (2009).

[38] C. Q. Wu, Phys. Rev. B. **113**, 4204 (1993).

[39] H. Zhao, Y.-G. Chen, X.-M. Zhang, Z. An, and C.-Q. Wu, J. Chem. Phys. **130**, 234908 (2009).

[40] Y. Meng, B. Di, X. J. Liu, Z. An, and C. Q. Wu, J. Chem. Phys. **128**, 184903 (2008).

[41] Y. Meng, B. Di, X. J. Liu, Z. An, and C. Q. Wu, Eur. Phys. Lett. **79**, 17002 (2007).

[42] H. Ma and U. Schollwöck, J. Chem. Phys. **129**, 244705 (2008).

[43] H. Ma and U. Schollwöck, J. Phys. Chem. A. **114**, 5439 (2010).

[44] H. Ma and U. Schollwöck, J. Phys. Chem. A. **113**, 1360 (2009).

[45] Y. L. Zhang, X. J. Liu, Z. Sun, and Z. An, J. Phys. Chem. C. **118**, 2963 (2014).

[46] Y. L. Zhang, X. J. Liu, Z. Sun, and Z. An, J. Chem. Phys. **138**, 174906 (2013).

[47] Z. Sun, Y. Li, S. J. Xie, Z. An, and D. S. Liu, Phys. Rev. B. **79**, 201310(R) (2014).